Supplementary Materials and Methods.

Surface Plasmon Resonance (SPR).

The Activin A mAb was tested for binding cross-reactivity to a panel of TGF-beta family members, measurements were performed on a Biacore 4000 instrument using a dextran-coated (CM4) chip at 37°C. A capture sensor surface was prepared by covalently immobilizing monoclonal mouse anti-human Fc antibody (GE Healthcare, Piscataway, NJ) to the chip surface using (1-Ethyl-3-[3-dimethylaminopropyl]carbodiimide hydrochloride)/N-hydroxysuccinimide (EDC/NHS) coupling chemistry. Following surface activation, anti-human Fc antibody in coupling buffer (0.1 M acetate buffer, pH 4.5) was injected over the activated chip surface until a resonance unit (RU) signal of about 8000 RU (anti-human Fc antibody) was reached. The activated coupled chip surfaces were then washed and treated with 10 mM glycine-HCl, pH 1.5, to remove uncoupled residual proteins. The biacore running buffer was filtered HBS-T (0.01 M HEPES pH 7.4, 0.5 M NaCl, 3 mM EDTA, 0.5 mg/ml bovine serum albumin, 0.05% v/v Surfactant P20).

The Activin A mAb, Acvr2b-hFc or an isotype control antibody were captured on a monoclonal mouse anti-human Fc antibody (GE). Capture levels ranging from 60-200 resonance units (RUs) were obtained for each of the antibodies or the soluble receptor. TGF-beta family ligands (R&D Systems) were injected for 3 minutes over the reference and captured antibody surfaces at concentrations ranging from 3.1 nM to 200 nM. Dissociation was monitored for 2 min and all capture surfaces were regenerated with one 15-s pulse of 10 mM glycine–HCl pH 1.5.

Measurement of serum Activin A levels after tamoxifen administration.

Ten week old wild type mice were injected intraperitoneally with 40mg/kg of tamoxifen daily for 8 days. Mice were injected intravenously with 1.7U of heparin 5 minutes before collecting blood. Activin A was measured in serum by an acid/SDS denaturing ELISA. Briefly, 20µl of samples were denatured using 180µl of 300 mM acetic acid/0.2%SDS for 10 minutes at room temperature, followed by neutralization with 200µl of 300 mM Tris/ 2%BSA/ 2%Triton-X-100 before being analyzed by a standard ELISA protocol.

Supplementary Figures:

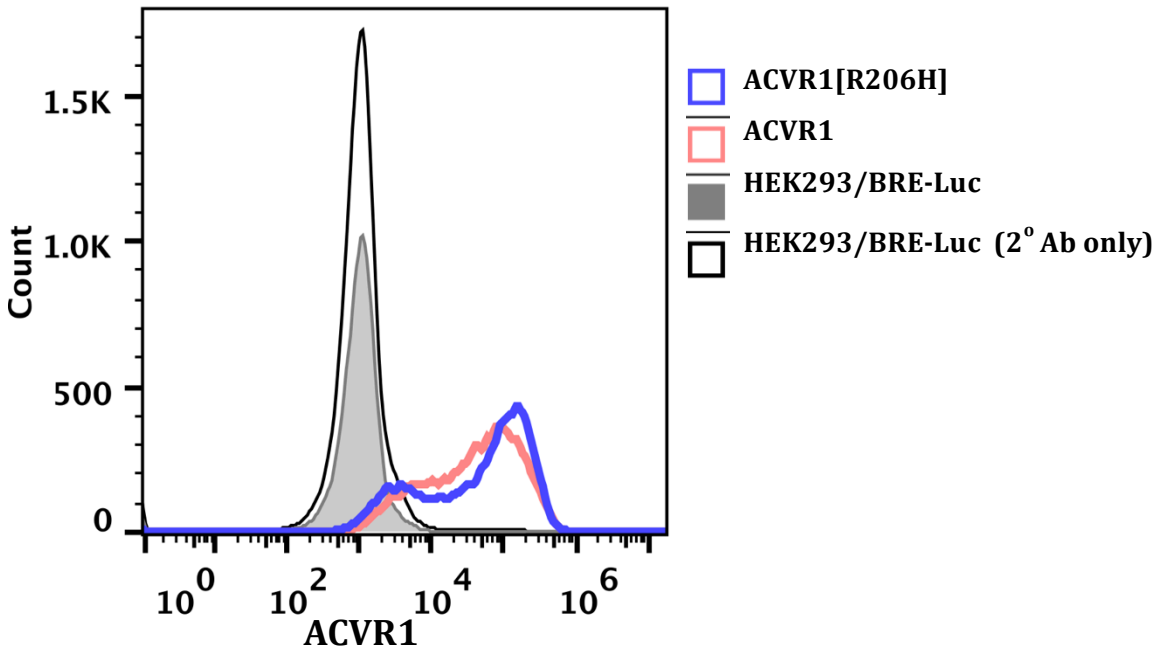

Fig. S1. Expression of ACVR1 in HEK293/BRE-Luc cells is detected by surface staining. Surface Expression of ACVR1 is detected in ACVR1 and ACVR1[R206H] transfected HEK293/BRE-Luc reporter cells after one round of FACS sorting. Live cell staining and FACS analysis of HEK293/BRE-Luc reporter cells with MAb637 shows that transfected cells stably overexpress ACVR1 on the cell surface. Staining is not above the level of the 2° antibody alone in the parental HEK293/BRE-Luc cells.

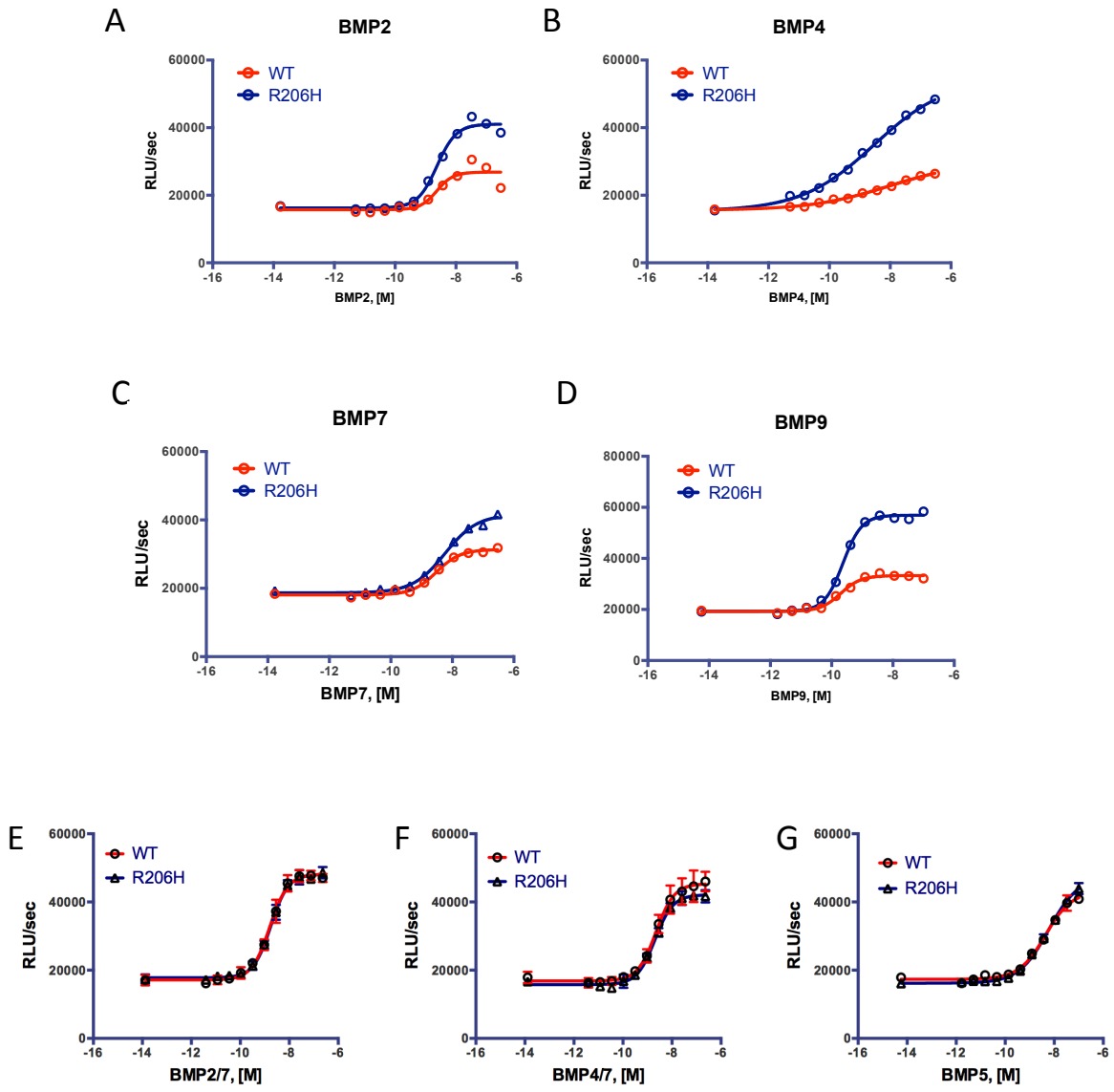

Fig. S2. Dose response curves of ACVR1 and ACVR1[R206H] overexpressing lines. (**A-D**) HEK293/BRE-Luc reporter cells overexpressing either wild type ACVR1 (WT; red circles) or ACVR1[R206H] (R206H; blue triangles) were treated with (**A**) BMP2, (**B**) BMP4, (**C**) BMP7 and (**D**) BMP9. Reporter lines expressing ACVR1[R206H] show enhanced signaling in response to these ligands. (**E-G**) In contrast, signaling initiated by (**E**) BMP2/7, (**F**) BMP4/7, and (**G**) BMP5, does not differ between ACVR1 and ACVR1[R206H]. Error bars represent standard deviation from samples run in triplicate. Lowest concentration on dose response represents no addition of ligand.

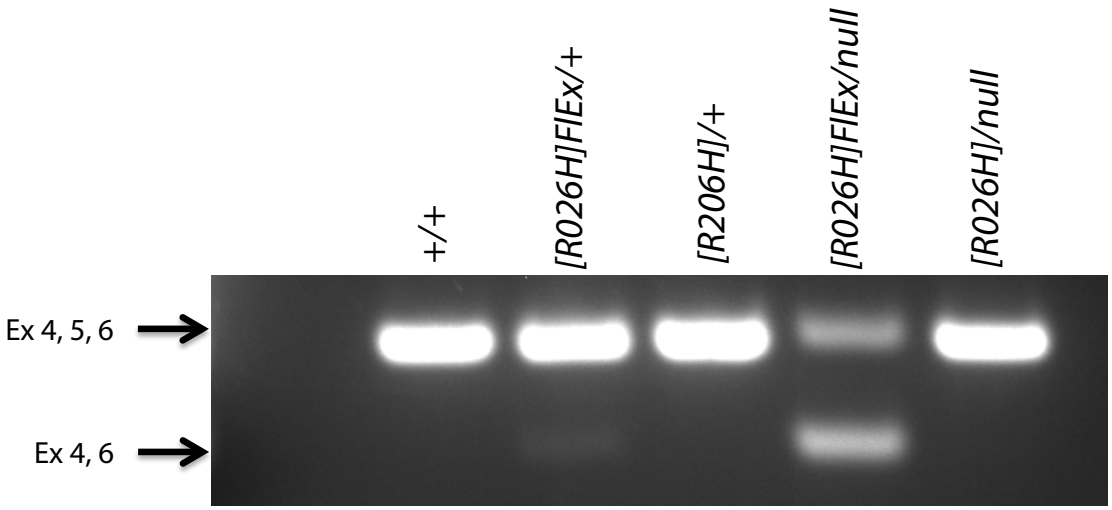

Fig. S3. *Acvr1* Exon 5 can skipped during splicing of the *Acvr1*$^{[R206H]FlEx}$ pre-mRNA. Mouse *Acvr1*$^{[R206H]FlEx/+}$*; Gt(ROSA26)Sor*$^{CreERT2/+}$ and *Acvr1*$^{[R206H]FlEx/null}$*; Gt(ROSA26)Sor*$^{CreERT2/+}$ ES cells were treated with 100 nm Tamoxifen for 24hrs to induce inversion of the [R206H]-containing exon into the sense strand and effectively convert *Acvr1*$^{[R206H]FlEx}$ into *Acvr1*$^{[R206H]}$. RNA was isolated from *Acvr1*$^{+/+}$ (+/+), *Acvr1*$^{[R206H]FlEx/+}$ (*[R206H]FlEx/*+), *Acvr1*$^{[R206H]/+}$ (*[R206H]/*+), *Acvr1*$^{[R206H]FlEx/null}$ (*[R206H]FlEx/null*), and *Acvr1*$^{[R206H]/null}$ (*[R206H]/null*). RT-PCR was performed to amplify exons 4 through 6. The RT-PCR product was analyzed on a 2% Agarose gel. Note the presence of a lower size band (Ex4, 6) that is consistent with exclusion of exon 5 from the mRNA in the *Acvr1*$^{[R206H]FlEx/+}$ and *Acvr1*$^{[R206H]FlEx/null}$ lines. Sequence analysis of the splice junction verified that exon 5 was absent in the lower band in the *Acvr1*$^{[R206H]FlEx/+}$ and *Acvr1*$^{[R206H]FlEx/null}$ lines.

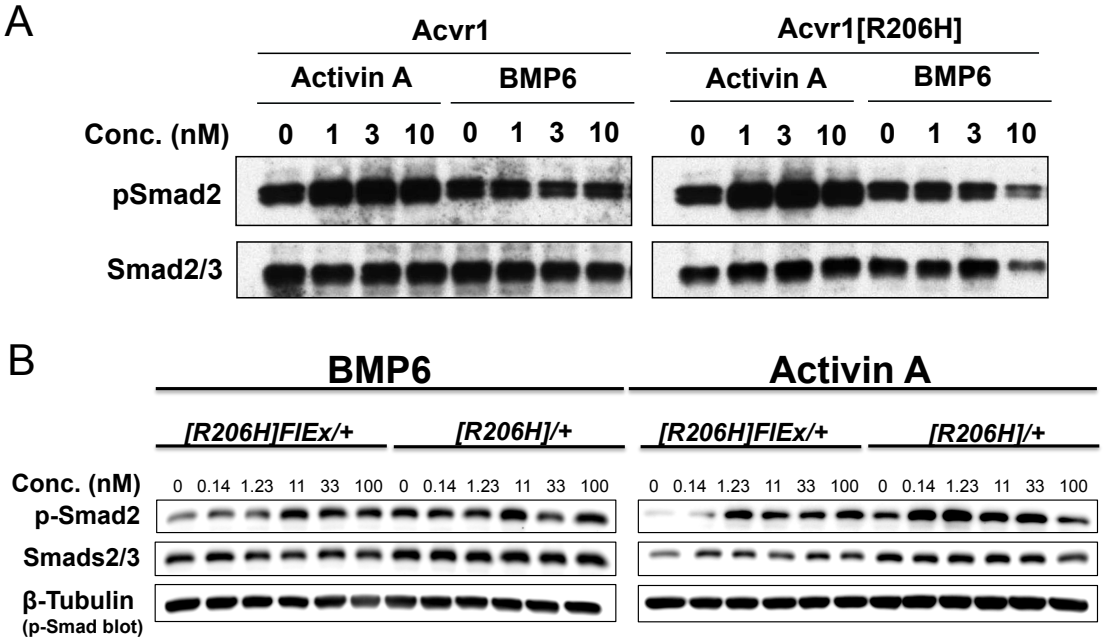

Fig. S4. Activin A-induced Smad2/3 signaling in ACVR1[R206H]-expressing cells. (**A**) Smad2/3 phosphorylation in response to Activin A or BMP6 in HEK293/BRE-Luc reporter lines expressing either ACVR1 or ACVR1[R206H]. (**B**) Smad2/3 phosphorylation in response to Activin A or BMP6 in *Acvr1*$^{[R206H]FlEx/+}$*; Gt(ROSA26)Sor*$^{CreERT2/+}$ (*[R206H]FlEx/+*) and tamoxifen-treated *Acvr1*$^{[R206H]/+}$*; Gt(ROSA26)Sor*$^{CreERT2/+}$ (*[R206H]/+*) mouse ES cells.

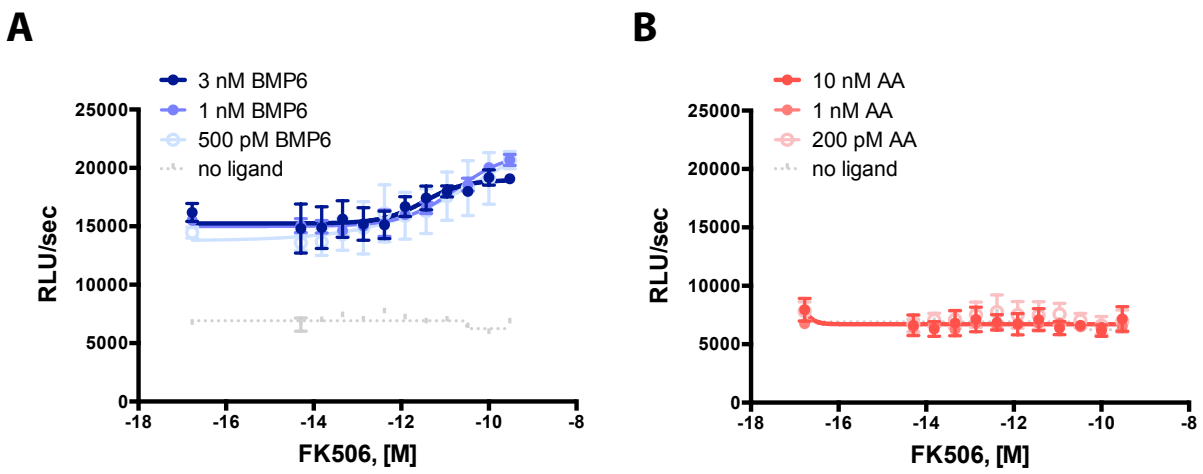

Fig. S5. FKBP12 inhibition by FK506 does not render wild type ACVR1 into an Activin-responsive receptor. HEK293/BRE-Luc reporter cells overexpressing wild type ACVR1 were treated with (**A**) 500 pM, 1 nM and 3 nM BMP6 or (**B**) 200 pM, 1 nM and 10 nM Activin A (AA). Simultaneously, FK506 was added in increasing amounts. FK506 boosts BMP6 signaling but does not enable a Smad1/5/8-based response to Activin A. Error bars represent standard deviation from samples run in triplicate. Lowest concentration on dose response represents no addition of FK506.

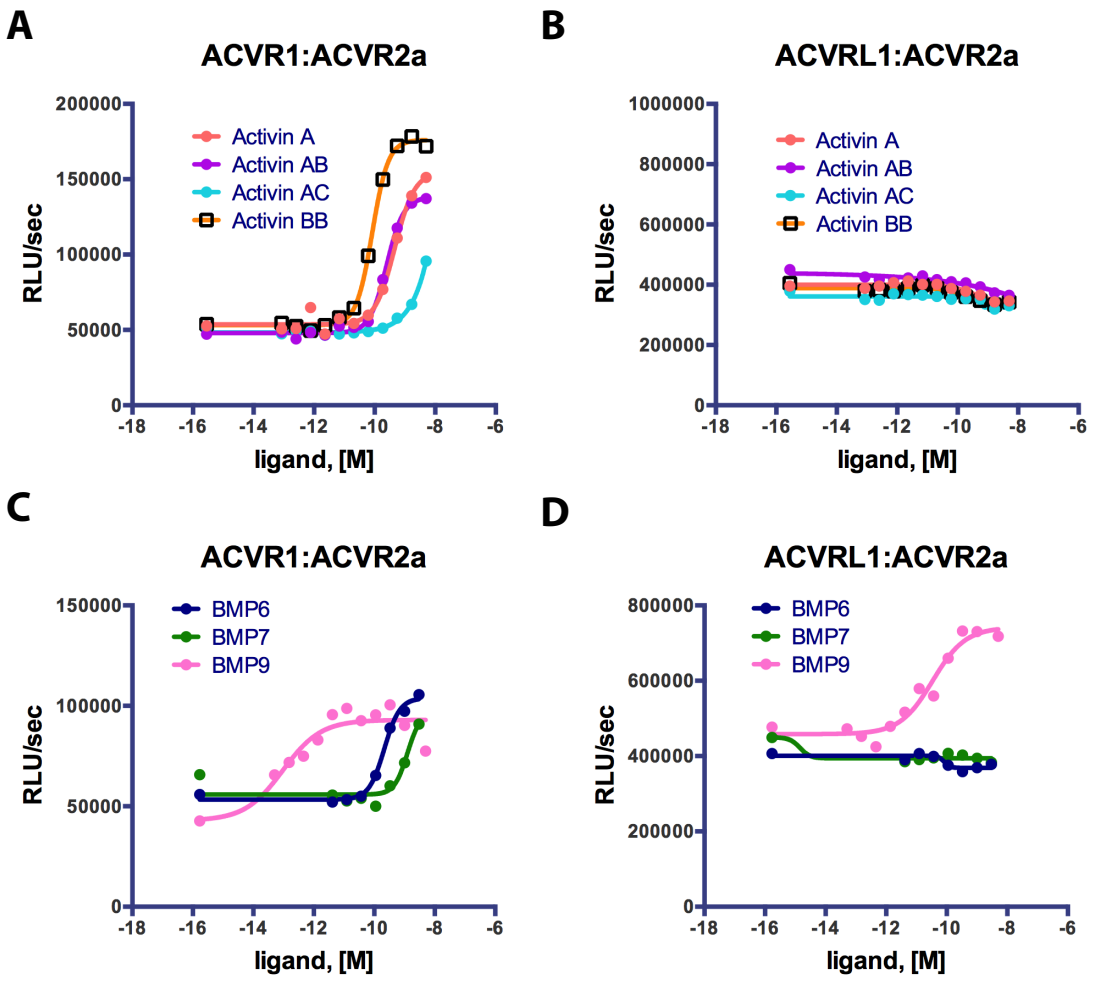

Fig. S6. Activins and BMPs bind to wild type ACVR1 and form complexes with ACVR2A. Exogenous BMP and Activin ligands were added to a LacZ complementation system in U20S cells (DiscovRx). (**A**, **C**) The data shows that BMP6, BMP7, BMP9 and Activins can dimerize ACVR1 and ACVR2A in these lines. (**B**, **D**) Only BMP9 induces dimerization of ACVRL1 (the closest homolog of ACVR1) with ACVR2A. (The lowest concentration on dose response represents no addition of ligand.)

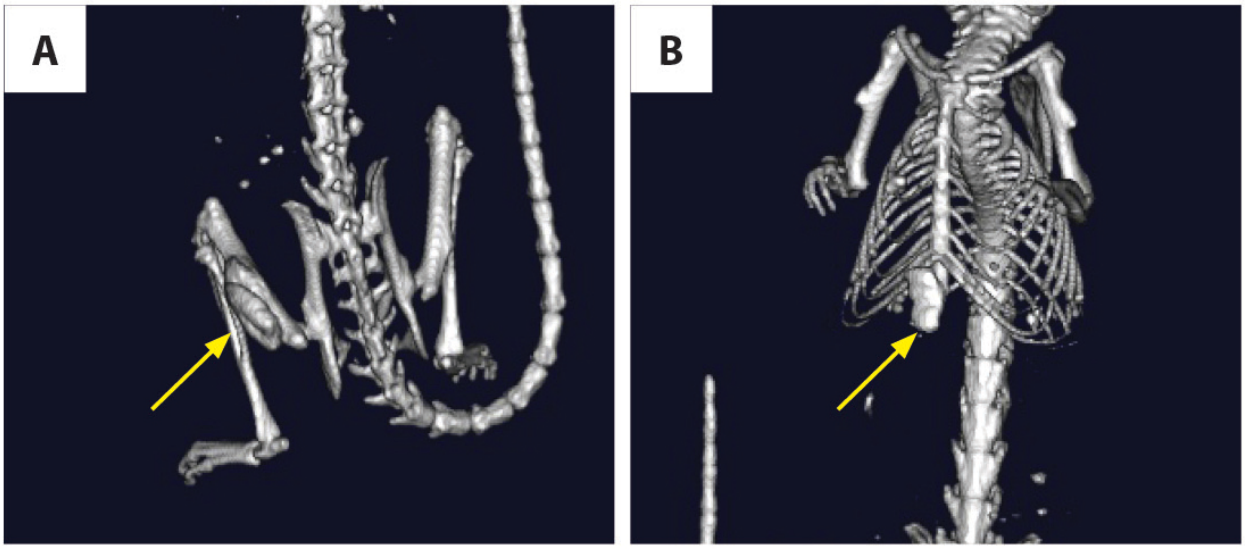

Fig. S7. ***Acvr1*** $^{[R206H]FlEx/+}$ ***; Gt(ROSA26)Sor*** $^{CreERT2/+}$ **mice develop HO as early as two weeks after tamoxifen administration.** Examples of *in vivo* μCT images of mice two weeks after initiation of treatment with tamoxifen. HO was found in (**A**) the hindlimb and (**B**) the sternum.

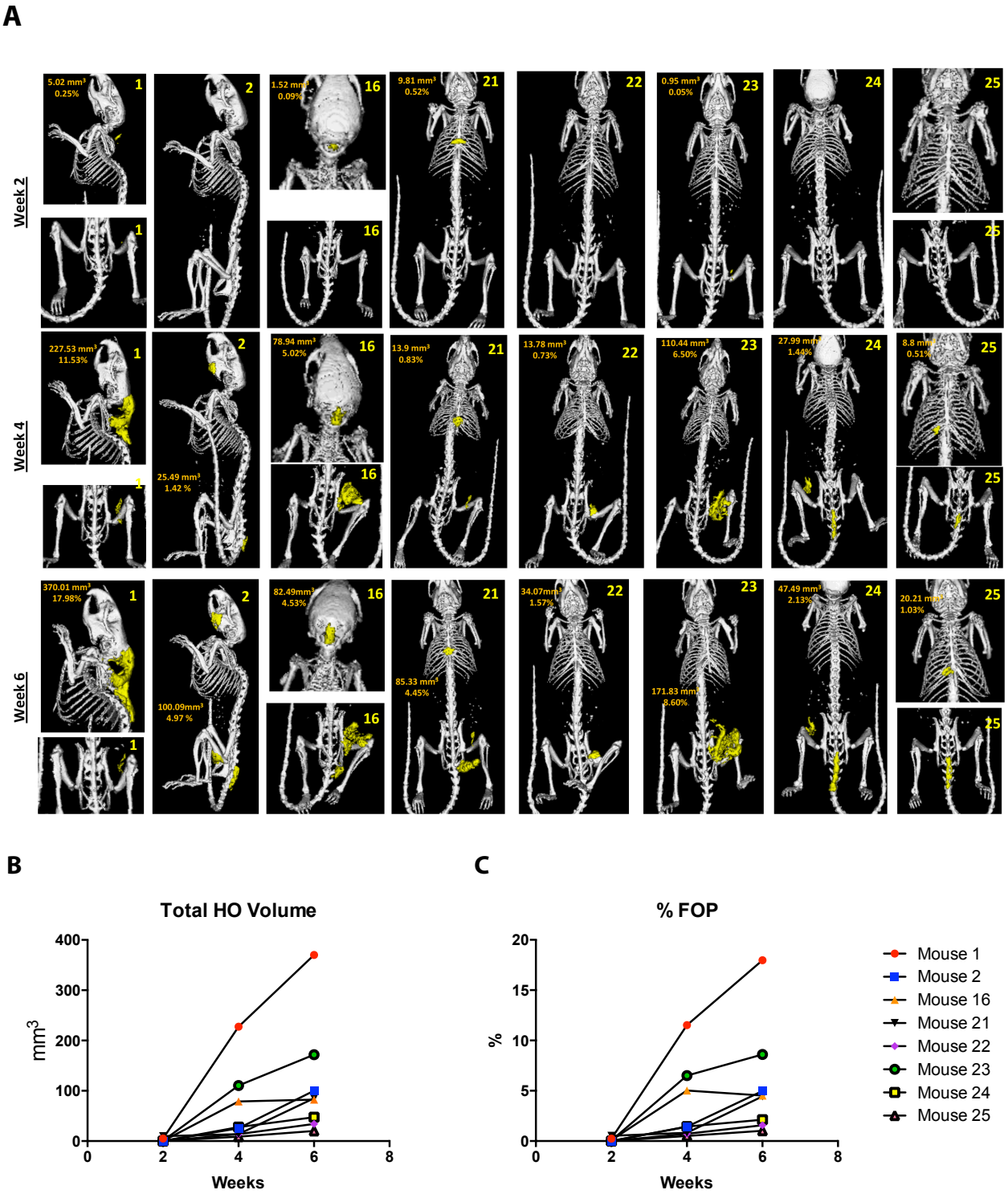

Fig. S8. Quantification of HO formation *Acvr1*$^{[R206H]FlEx/+}$; *Gt(ROSA26)Sor*$^{CreERT2/+}$ mice from two to six weeks after tamoxifen administration. (A) *in vivo* μCT images of mice two, four and six weeks after initiation of treatment with tamoxifen. HO was segmented from the skeleton (yellow) and quantified. (B) The total amount of HO in mm^3 in individual mice over a 6 week period. (C) The percentage of total bone volume that is HO in each mouse over a 6 week period.

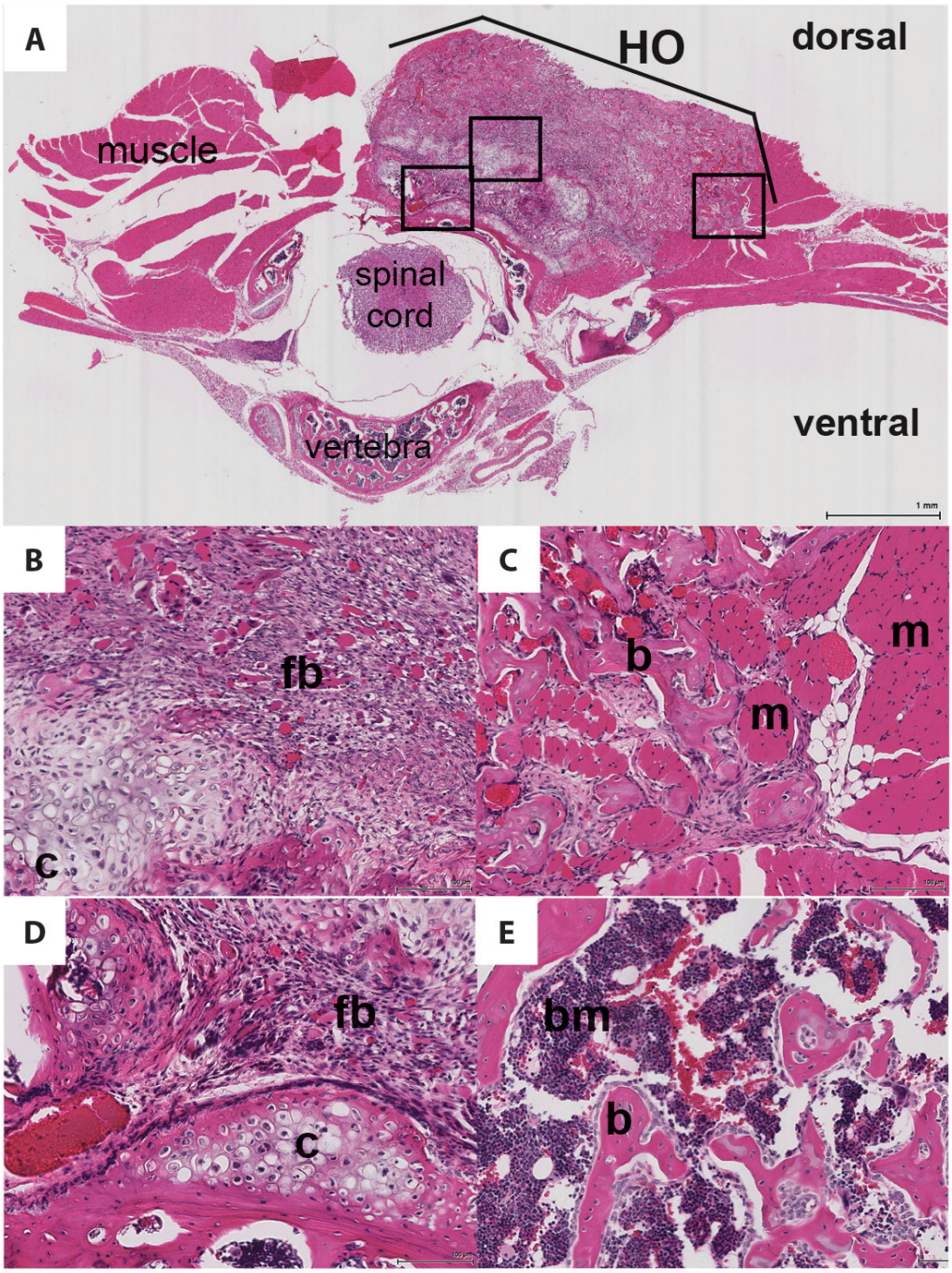

Fig. S9. H&E sections from HO lesions shows a variety of different cell types. (**A**) Transverse section through the vertebrae with a developing HO lesion on the left dorsal side. (**B**) chondrocytes (c) and fibroblasts (fb) are present in the HO. (**C**) Trabecular-like bone structures (b) are interspersed between muscle fibers (m). (**D**) Evidence of fusion of newly developing cartilage (c) and bone with the existing bones of the rib. (**E**) More mature region of HO that looks similar to normal bone (b) and is filled with bone marrow (bm).

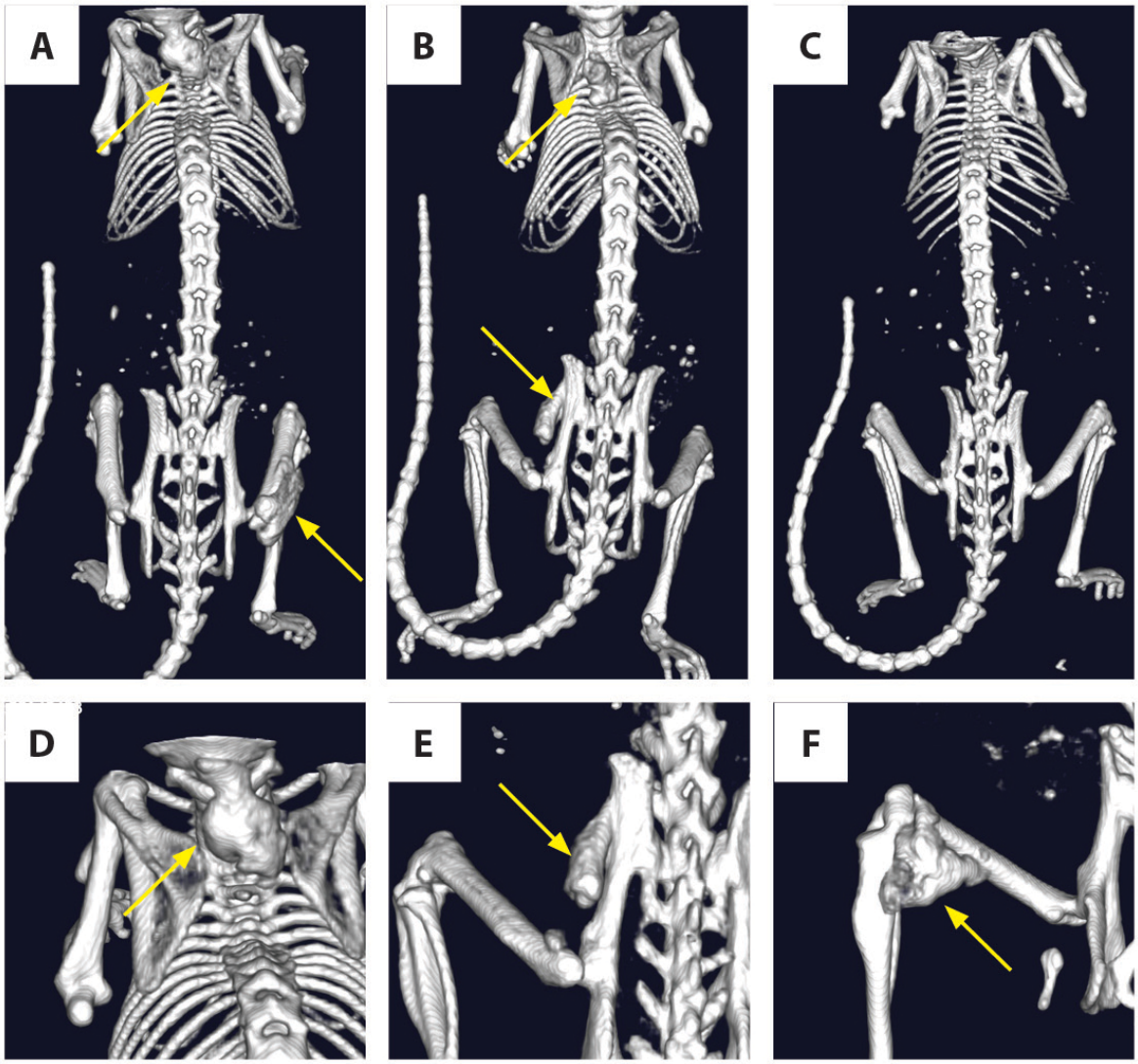

Fig. S10. ACVR2A-Fc and ACVR2B-Fc prevent ectopic bone formation in *Acvr1*$^{[R206H]FlEx/+}$; *Gt(ROSA26)Sor*$^{CreERT2/+}$ mice. Representative *in vivo* μCT images of mice 4 weeks after initiation of the FOP model. (**A**, **B**) Treatment with Fc control (10 mg/kg, twice weekly), or (**C**) with a combination of ACVR2A-Fc and ACVR2B-Fc (10 mg/kg twice weekly). HO is found for example in the neck (**D**), hip (**E**) and knee (**F**) of Fc control treated mice.

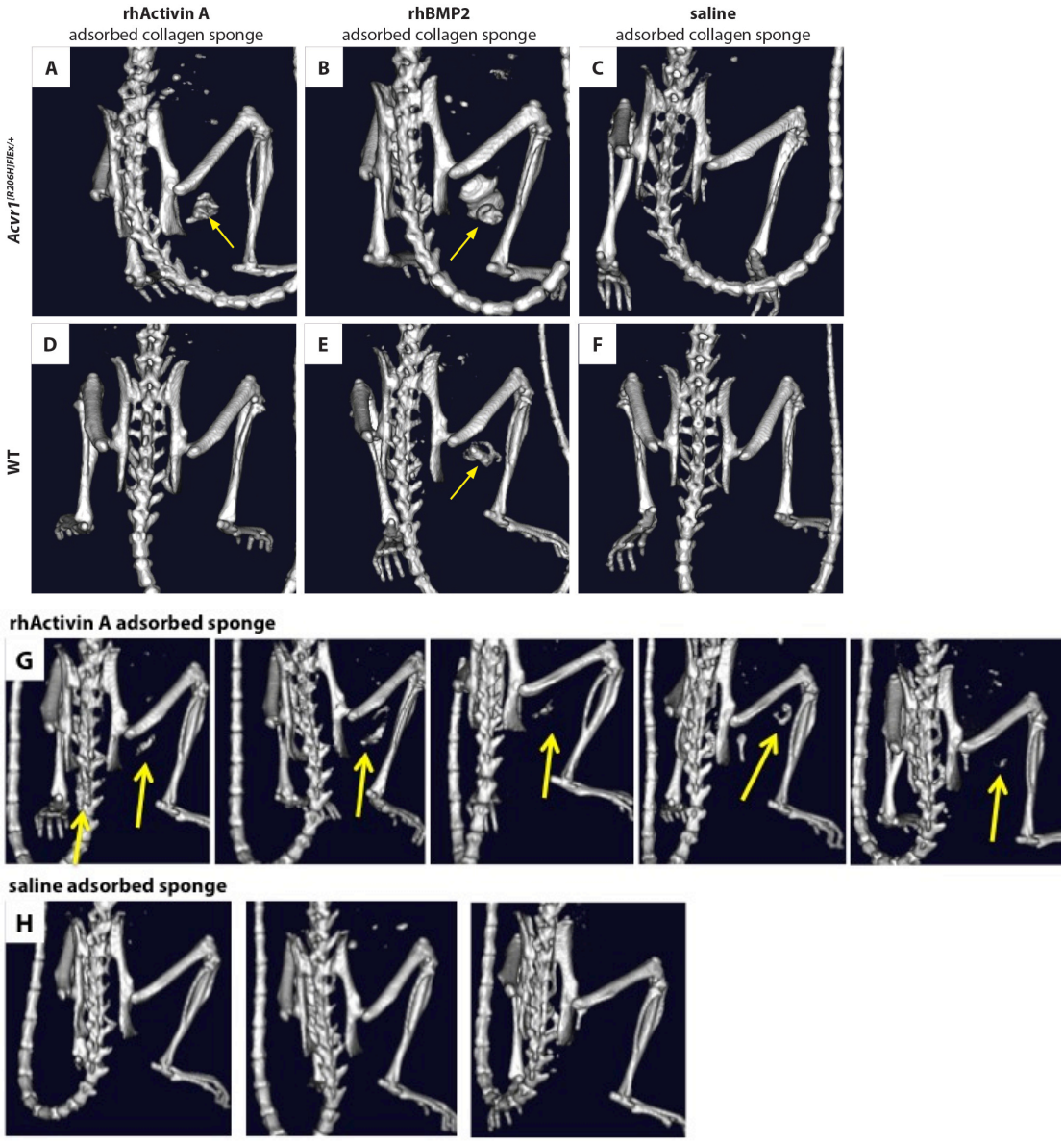

Fig. S11. Activin A causes HO in tamoxifen-treated *Acvr1*$^{[R206H]FlEx/+}$; *Gt(ROSA26)Sor*$^{CreERT2/+}$ but not wild type mice. *In vivo* μCT images of mice taken two weeks after implantation of collagen sponges adsorbed with Activin A (**A, D**) or BMP2 (**B, E**) or saline (**C, F**). In the Activin A-containing sponge implantations, HO (yellow arrows) was observed only in the tamoxifen-treated *Acvr1*$^{[R206H]FlEx/+}$; *Gt(ROSA26)Sor*$^{CreERT2/+}$ mice (**A**), and was absent from wild type mice (**D**). In contrast, HO is observed in both genotypes (**B, E**) in BMP2-containing sponge implantations group. No HO at the site of implantation was observed in both genotypes (**C, F**) in the saline group. **(G)** Activin A adsorbed sponges induced HO in tamoxifen treated *Acvr1*$^{[R206H]FlEx/+}$; *Gt(ROSA26)Sor*$^{CreERT2/+}$ mice previously receiving Acvr2a-Fc. Mice were treated with Acvr2a-Fc (10mg/kg twice weekly) for 7 weeks, followed by no treatment for 8 weeks and then implanted with either Activin A adsorbed **(G)** or saline adsorbed **(H)** sponges. HO was observed at the site of Activin A adsorbed sponge implantation **(G)** but not saline adsorbed sponges **(H)** at 2 weeks. HO was also detected in the tail of one mouse.

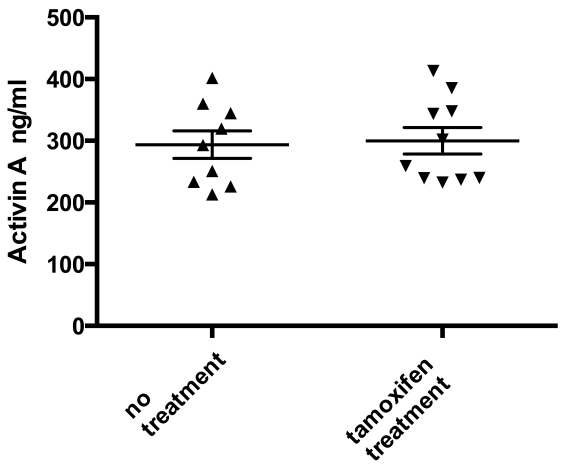

Fig S12. Tamoxifen does not alter serum Activin A levels. Activin A levels were measured by ELISA in serum from mice that were either untreated or treated with 40mg/kg of tamoxifen daily for 8 days.

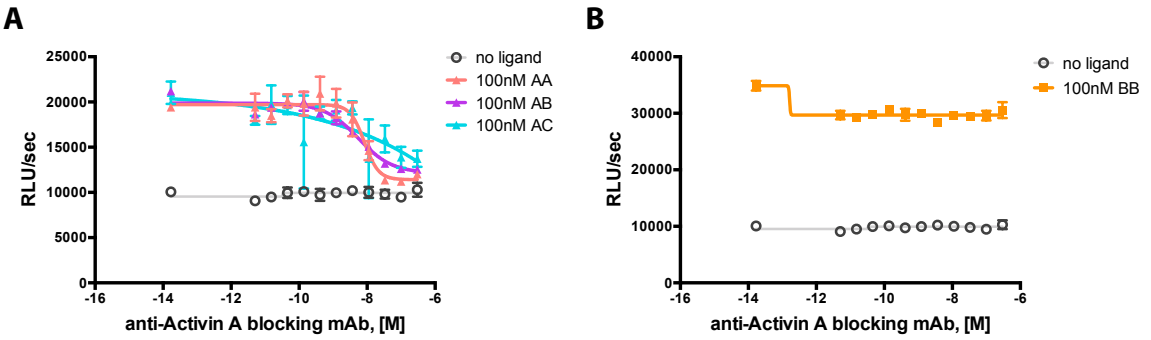

C

Ligand injected \ mAb captured ---->	Activin A mAb	Acvr2b-Fc	isotype control mAb
Activin A	53.2	70.9	-0.1
Activin B	2.6	68.0	1.9
Activin AB	66.7	59.5	-0.1
Activin AC	15.2	59.4	-0.1
hBMP2	3.3	36.9	-1.0
hBMP4	0.8	26.4	0.4
hBMP6	5.3	86.3	5.1
hBMP7	5.7	64.2	4.3
hBMP9	-0.3	32.3	-1.0
hBMP10	0.5	34.2	0.3
GDF8	0.7	25.8	0.5
GDF11	1.8	24.2	3.0
mBMP4	0.2	9.1	0.1
mBMP5	16.1	52.5	14.2
mBMP6	12.1	72.8	10.3
mBMP7	6.1	52.5	5.6
mBMP8a	2.8	5.6	0.3
mBMP9	0.4	21.7	0.1
mBMP10	1.3	27.9	1.3

Fig. S13. Anti-Activin A blocking mAb binds and blocks the activity of Inhibin A-containing Activins but not Activin B. (**A**) HEK293/BRE-Luc reporter cells overexpressing ACVR1[R206H] were treated with 100nM Activin A, Activin AB or Activin AC. A dose-dependent inhibition of BRE-driven, luciferase reporter signaling is observed with the anti-Activin A blocking mAb. (**B**) Activin B signaling in this line was not inhibited by the anti-Activin A blocking mAb. **(C)** The Activin A mAb was tested for binding cross-reactivity to a panel of TGF-beta family members by Biacore 4000 instrument. Resonance units (RUs) observed with 200 nM ligand injected over captured Activin A mAb, Acvr2b-Fc or isotype control mAb. The binding response of the captured Activin A mAb to the injected TGF-beta family ligands at 200 nM were compared to the RUs of a negative isotype control mAb, to provide a measure of background-level non-specific binding, and to the binding responses of Acvr2b-hFc, which was bound to all TGF-beta family members tested and therefore serves as a positive control ligand-binding. From this comparison, the Activin A mAb bound to Activin A, Activin AB, Activin AC but not appreciably to Activin B or to the BMP or GDF ligands.

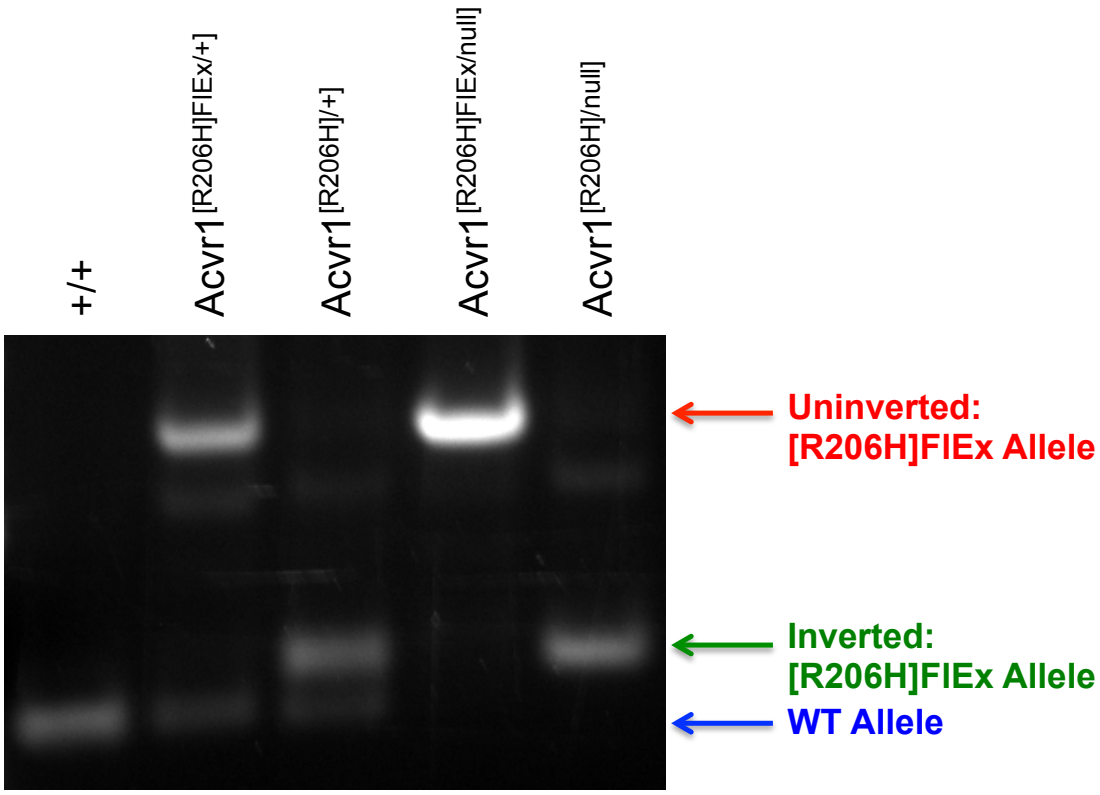

Fig. S14. In mouse ES cells, the *Acvr1*$^{[R206H]FlEx}$ allele is inverted by 24hr after 100nM Tamoxifen treatment. Genomic DNA was prepared from ES Cell cultures and PCR products from genomic DNA preparations were resolved on 2% Agarose gel. Upon addition of Tamoxifen, a band is observed representing the inverted [R206H]FlEx allele, ***Acvr1***$^{[R206H]}$.

Treatment	Isotype control	Acvr2a-Fc + Acvr2b-Fc	Acvr2a-Fc	Acvr2b-Fc	Activin A mAb
# mice with ectopic bone / total mice in group	36/38	1/11	2/15	0/7	0/22

Table S1. Number of mice with HO lesions in treatment experiments. The number of mice showing at least one HO lesion at 4 weeks post initiation of the model with tamoxifen detected by in vivo μCT out of the total number of mice receiving each treatment. Mice are pooled from multiple treatment experiments.

Genotype	Number pups	% pups
Acvr1$^{+/+}$	25	40%
Acvr1$^{[R206H]FlEx/+}$	38	60%
Acvr1$^{[R206H]FlEx/[R206H]FlEx}$	0	0%
Total	63	100%

Table S2. ***Acvr1***$^{[R206H]FlEx/+}$ **mice cannot be bred to homozygosity.** Genotypes of pups from nine litters from *Acvr1*$^{[R206H]FlEx/+}$ x *Acvr1*$^{[R206H]FlEx/+}$ crosses. No *Acvr1*$^{[R206H]FlEx/[R206H]FlEx}$ were identified indicating embryonic or perinatal lethality. Chi-squared test $p<0.0001$ (22.52)